



## The paleolandscape evolution of the southwestern coast of Sardinia (Italy) and its impact on Mesolithic settlements

Rita Teresa Melis, Valentino Demurtas, Margherita Mussi, Paolo Emanuele Orrù, Andrea Sulis, Flavio Altamura, Rosanna Erbi, Michele Orrù & Giacomo Deiana

**To cite this article:** Rita Teresa Melis, Valentino Demurtas, Margherita Mussi, Paolo Emanuele Orrù, Andrea Sulis, Flavio Altamura, Rosanna Erbi, Michele Orrù & Giacomo Deiana (2023): The paleolandscape evolution of the southwestern coast of Sardinia (Italy) and its impact on Mesolithic settlements, Journal of Maps, DOI: [10.1080/17445647.2023.2182722](https://doi.org/10.1080/17445647.2023.2182722)

**To link to this article:** <https://doi.org/10.1080/17445647.2023.2182722>



© 2023 The Author(s). Published by Informa UK Limited, trading as Taylor & Francis Group.



[View supplementary material](#)



Published online: 21 Mar 2023.



[Submit your article to this journal](#)



[View related articles](#)



[View Crossmark data](#)



This article has been awarded the Centre for Open Science 'Open Materials' badge.



## The paleolandscape evolution of the southwestern coast of Sardinia (Italy) and its impact on Mesolithic settlements

Rita Teresa Melis <sup>a</sup>, Valentino Demurtas <sup>a</sup>, Margherita Mussi <sup>b</sup>, Paolo Emanuele Orrù <sup>a</sup>, Andrea Sulis<sup>c</sup>, Flavio Altamura <sup>d</sup>, Rosanna Erbi<sup>e</sup>, Michele Orrù<sup>f</sup> and Giacomo Deiana <sup>a</sup>

<sup>a</sup>Department of Chemical and Geological Science, University of Cagliari, Cagliari, Italy; <sup>b</sup>ISMEO – Corso Vittorio Emanuele II, Roma;

<sup>c</sup>Department of Architecture, Design and Urban Planning, University of Sassari, Alghero, Italy; <sup>d</sup>flavioaltamura@libero.it; <sup>e</sup>rosanna.erbi@gmail.com; <sup>f</sup>mick823@hotmail.it

### ABSTRACT

We present a geomorphological map of the southwestern coast of Sardinia encompassing inland and offshore areas of the S'Ormu e S'Orku Mesolithic site. The submerged area was documented by high-resolution multibeam bathymetry combined with Side-Scan Sonar data. The emerged coastal area was surveyed using Uncrewed Aerial Vehicle Remote Sensing and field surveys. The inland landforms were shaped by coastal, fluvial, and gravity-induced processes. Most of the submerged landforms appear to be modeled in subaerial conditions during sea-level lowstands, and then sealed by the rising sea level. The coastal evolution has been characterized by the rapid cliff retreat facilitated intense linear erosion of watercourses, by debris flows, rockfalls and toppling. Geomorphological evidences of cliff retreat due to landslide was supported by a simplified analytic hydraulic model of the wave-cliff interaction. These processes and the sea level rise canceled any possible Mesolithic settlement along the coast. The survival of the S'Ormu e S'Orku site is only due to a protected morphological position and to the distance from the Early Holocene coastline. The dearth of coastal Early Holocene prehistoric sites is likely the outcome of the presented coastal dynamics.

### ARTICLE HISTORY

Received 21 November 2022

Revised 2 February 2023

Accepted 15 February 2023

### KEYWORDS

Cliff retreat; abrasion platform; rockfalls; Pleistocene; Holocene; geomorphological mapping; morphostratigraphy

## 1. Introduction

During the low stands of MIS 2 Sardinia was joined to Corsica and the Sardo-Corsican landmass was the largest Mediterranean island (Palombo et al., 2017). Then the strait of Bonifacio opened, splitting this landmass in the two islands. In the final Late glacial the sea level rapidly rose and the coastal morphology markedly changed. The shorelines were exposed to the impact of wave action and marine currents (Bailey & Cawthra, 2021). Consequently, much of the coastal landscape and related prehistoric record have since been eroded or submerged (Ammerman, 2020; Bailey & Cawthra, 2021; Castagnino Berlinghieri et al., 2020; Chelli et al., 2018; Galanidou et al., 2020; Galanidou & Bailey, 2020; Galili et al., 2020; Gambin, 2020; Geoff et al., 2020; Geoff et al., 2020; Putignano et al., 2014; Radić Rossi et al., 2020; Skaarup & Grøn, 2004).

Focusing on the southwestern coast of Sardinia (Figure 1(a,b)), here we present background information on the impact of sea-level rise and coastal changes (Orrù et al., 2011, 2014; Ulzega et al., 1986). We produce a geomorphological map of the submerged area to reconstruct the coastal morphogenetic

evolution. In stable areas, the submersion of a gently dipping coast can be calculated using the known rise of sea level. The quantification of retreat rates on rocky coasts is more complex as there are many factors and variables (Del Río & Gracia, 2009; Duguet et al., 2021; Furlani et al., 2014; Young, 2018). We underline that soft rocks cliffs, which characterize the study area, are particularly exposed to marine processes, resulting in a fast retreat of the coastline. Our aim is also to estimate the cliff retreat since the Early Holocene.

Coastlines probably were attractive environments for prehistoric human groups exploiting the many available resources (Bailey & Flemming, 2008). Molluscs and fish could be caught in the intertidal areas while flat stretches next to the shore allowed easy movement. Such sites are rare along the northern coasts of the Mediterranean. This is also the case of islands, where the rising sea level and related coastal evolution played an important role in human peopling (Benjamin et al., 2017). In Sardinia, there is no firm prehistoric evidence before the Early Holocene, when a sparse number of sites occur inland (Martini & Tozzi, 2012). The most relevant one is the S'Ormu

**CONTACT** Valentino Demurtas valentino.demurtas@unica.it Department of Chemical and Geological Science, University of Cagliari, Monserrato 09042, Italy

Supplemental data for this article can be accessed online at <https://doi.org/10.1080/17445647.2023.2182722>.

© 2023 The Author(s). Published by Informa UK Limited, trading as Taylor & Francis Group.

This is an Open Access article distributed under the terms of the Creative Commons Attribution License (<http://creativecommons.org/licenses/by/4.0/>), which permits unrestricted use, distribution, and reproduction in any medium, provided the original work is properly cited. The terms on which this article has been published allow the posting of the Accepted Manuscript in a repository by the author(s) or with their consent.



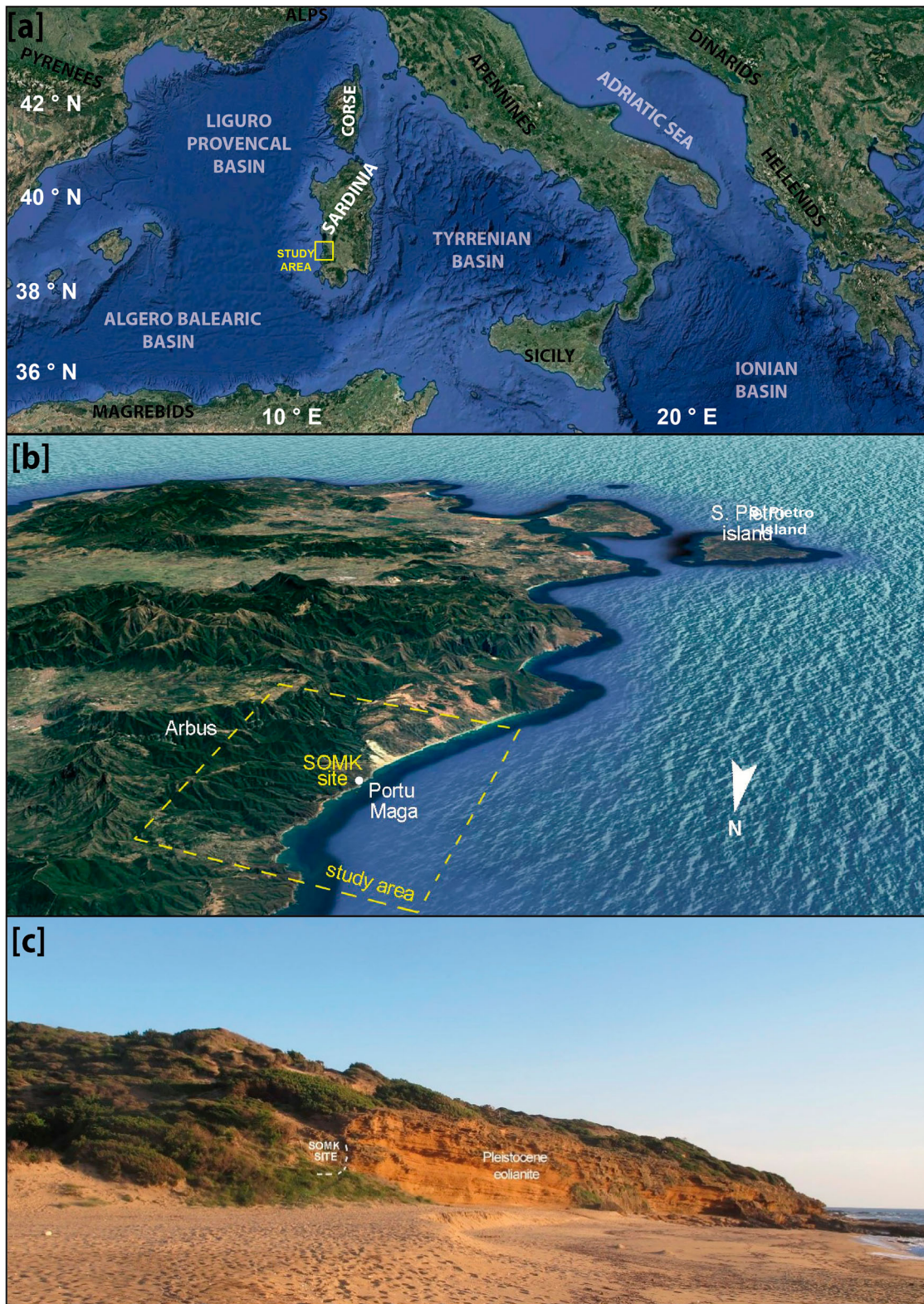


**Figure 1.** Geographical location of the study area modified after Demurtas et al. (2021a); (b) In yellow the main map area and the location of the SOMK site; (c) a view of the SOMK site.

e S'Orku (SOMK) (Figure 1(b,c)), the only coastal Mesolithic site. It is located along the southwestern coast at the base of an eolianite cliff just a few meters from the modern shoreline.

To evaluate the actual presence or absence of sites a detailed reconstruction of paleo-coastal systems and the assessment of coastal dynamics are both needed. The current study is relevant to understand their

role in possibly making Mesolithic sites disappear from vast stretches of Sardinia.

## 2. Study area

The study area is near Portu Maga (Arbus), on the southwestern coast of Sardinia. The coastal strip is currently characterized by 5–10 m high cliffs, with



scattered sandy pocket beaches and little bedrock promontories.

The coast is bounded inland by reliefs incised by deep valleys on the Variscan metamorphic basement, mainly represented by metasandstones, fossiliferous metasyllites and metargillites (San Vito Formation, upper-middle Ordovician) (Carmignani et al., 2015). During the Pleistocene, sea level fluctuations led to the deposition of littoral and continental sediments, which crop out extensively along most of the coast.

At the local scale, at the base, there are littoral deposits mainly consisting of polygenic and heterometric conglomerates with an arenaceous matrix and a high fossiliferous content dominated by *Glycymeris*, *Patella ferruginea* and *Arca* (Palmerini & Ulzega, 1969), in turn often fossilized by biogenic limestones at Lithothamnium. These deposits rest on a marine wave-cut platform; comparisons with deposits cropping out further north suggest that they are of MIS 5 age (Deiana et al., 2021a; Ferranti et al., 2006).

After the Last Interglacial, eolian dune bodies formed, as shown by cross-laminated sandstones (eolianites). They are evidence of coastal retreat and are followed by paleo-riverbed summit levels and loess deposits. As in the central and northwestern coast of Sardinia (Andreucci et al., 2010), we date the whole complex to MIS 4/3.

Stratified slope deposits with cryoclastic (*éboulis ordonnés*) deposits are embedded in the eolian cross-laminated sandstones. We date them to the peak of the Last Glacial Maximum which corresponds to the regressive maximum at -125 / -130 meters (Deiana et al., 2021; Orru et al., 2012). Holocene eolian deposits and thick layers of debris slope cover the Pleistocene deposits.

The Mesolithic site of SOMK (5 m a.s.l.) is a collapsed rockshelter in the eolianite cliff near the mouth of the S'Ormu e S'Orku stream. Burials were discovered within a complex lithostratigraphic sequence dated between ca 9000 and 8000 years cal BP (Melis & Mussi, 2016). They include the ochrestained skeleton of an adult male accompanied by a large *CharonIa lampas* shell. Obsidian and jasper were used to produce lithic tools. Obsidian is abundantly found inland, while jasper outcrops nearby in the now San Pietro island which at the time was joined to the mainland (Deiana et al., 2021). The Mesolithic groups could move along a flat sandy coastal strip with dunes and lagoons.

The local meteorological and marine climate is strongly influenced by the periodic passage of mesoscale anticyclones across the Northern Mediterranean Sea, which generates strong Mistral winds blowing south-eastwards from the Gulf of Lion to the Sicilian Channel. Wind velocities are generally approximately 3 m/s, but velocities as high as 10 m/s are not uncommon.

### 3. Methods

#### 3.1. Geological geomorphological surveys

Multiscale geological and geomorphological surveys were performed using field survey and remote sensing analysis. A remote sensing survey through the interpretation of multi-temporal aerial photos (Autonomous Region of Sardinia since 1954–2019) was carried out. Digital terrain models (LiDAR data of 1-m cell size, Autonomous Region of Sardinia, 2008) were used.

The main map was created using the Esri ArcGIS/ArcMap using the 1-m cell size DTM of the Autonomous Region of Sardinia at 1:10,000 scale for the inland area, while for the submerged area we used side scan sonar data and EMODNET dtm.

It was produced integrating various approaches. The submerged study area was analyzed using EMODNET multibeam bathymetry combined with Side-Scan Sonar data (Deiana et al., 2021, 2022). The emerged coastal area was surveyed using Uncrewed Aerial Vehicle Remote Sensing and field surveys data.

UAV Digital photogrammetry is a good tool to analyze rocky slopes and perform morphometric analysis (Deiana et al., 2021; Demurtas et al., 2021b; Muñoz Narciso et al., 2017). To analyze the cliff landslide, we used high-resolution digital elevation models acquired by structure from motion (Sfm) from UAV and terrestrial photogrammetry (Figure 2). Data mission acquisition was performed in September 2019 and January 2022 using the same acquisition parameters, drone and weather conditions.

Side-scan sonar data acquisition was performed on the proximal continental shelf with depths ranging from 15 to 50 m as part of the 'Mapping of *Posidonia oceanica* meadows along the coasts of 2001 Sardinia' project funded by the Italian Ministero dell'Ambiente on R/V 'Copernaut Franca'.

#### 3.2. Soft rock cliff recession analysis

**The rapid recession of soft cliffs has recently attracted considerable attention from civil engineers that have developed simplified models of the** multiple factors that control the process (Brooks et al., 2012; Castedo et al., 2012; Sunamura, 1982, 1992; Sulis and Annis, 2014, 2015). Sunamura (2012) provided a state-of-the-art review about present-day recession processes on soft-rock cliffed coasts (Del Río et al., 2020), developing and applying a model derived from the reanalysis of previously published data. In this paper, an improvement of Sunamura's model is proposed and applied to the cliff of Portu Maga. The mechanisms of cliff toe erosion is based on the comparison between two forces: the assailing

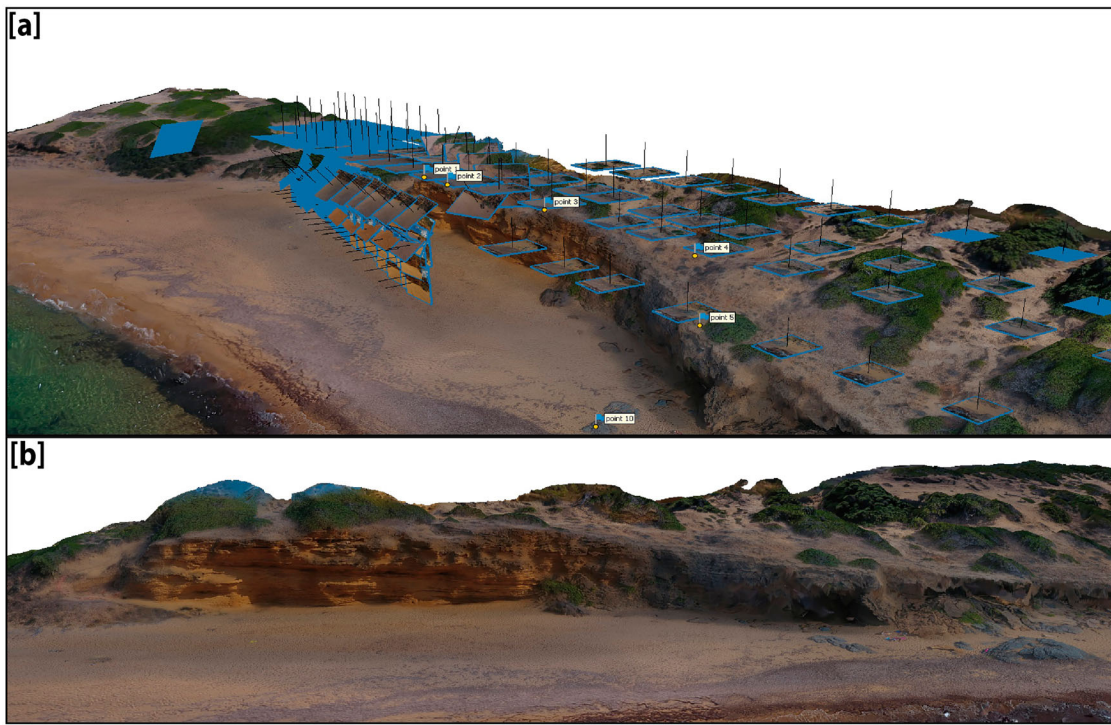


**Figure 2.** (a) UAV photos and Ground Control Points (GCP) processed in Metashape. Blue squares represent the oriented photos, the flags indicate the location of GCP, the model is the dense cloud. (b) 3D Tiled model of the cliff under study.

force of waves ( $F_w$ ) and the resisting force of rocks ( $F_R$ ). Erosion occurs only when the assailing wave force surpasses the rock-resisting force.

Sunamura's model:

- assumes that variables  $F_w$  and  $F_R$  are known with no random deviations;
- uses simplified mathematical conceptualization of the mechanisms;
- uses the same average value of parameter for the whole cliff;
- considers a single, measured or generated, storm.

The  $F_R$  of the sea cliff rock is determined by the mechanical strength of the material without discontinuities. Compressive strength, a widely used index with well-established testing criteria, is an appropriate parameter for the resisting force of rocks:

$$F_R = BS_C \quad (1)$$

where  $S_C$  is the compressive strength (Budetta et al., 2000) and  $B$  is a dimensionless coefficient.

$F_w$  at the cliff toe exerts two kinds of actions on its face—a hydraulic and a mechanical one. Hydraulic action of compression and tension can be determined from analytical formulations and is the only component that can be evaluated in this approach. Little is known about how to evaluate the fatigue limit of a rock mass under the action of waves in the field. Sunamura (2015) examined the  $F_w$  of laboratory breaking waves. He derived the force from the kinetic energy of water particles at the crest of breaking waves against

the cliff face as:

$$F_W = A\rho gH_{s,f} \quad (2)$$

where  $H_{s,f}$  is the significant wave height at the cliff toe,  $g$  the gravitational acceleration,  $\rho$  the water density and  $A$  a dimensionless coefficient. Here we processed wave data from an oceanographic buoy of the Italian Data Buoy Network (RON) (latitude = 40°33'11" N; longitude = 08°07'00" E). The available time series covers the period between July 1989 and April 2008. The extreme wave analysis (EWA) of the geographic transposed data was performed with the Weibull distribution and estimated with the least square method (Sulis et al., 2017).

Here a susceptibility index to erosion is defined as:

$$SI = \frac{F_W}{F_R} = \frac{A\rho gH_{s,f}}{B\sigma_c} \quad (3)$$

In this paper  $B$  is closely associated with the structures, and the presence of discontinuities such as cracks, joints, faults, and bedding planes were accurately surveyed. This allowed to estimate the effect produced by discontinuities on compressive strength reduction, through compression tests by crushing rock specimens. The Rock Mass index  $RMi$  (Palmström, 1996), has been developed in order to characterize the rock masses strength. It describes the method of determining the  $RMi$  for a rock mass using various common field observations and provides a measure of the reduction of intact rock strength caused by discontinuities, given by  $RMi = B \cdot \sigma_c$ .

### 3.3. Geoarchaeological survey and dating

The stratigraphic sequence of SOMK has been sampled and described during the excavation campaigns (2007–2022) which also yielded burials, lithic stone tools and faunal remains. Radiocarbon dating was made on coal and bone fragments in the INNOVA laboratory (Caserta) and NSF Tucson Arizona, and calibrated with CALIB Radiocarbon Calibration Version 8.2 html (Stuiver & Reimer, 1993).

## 4. Results

### 4.1. Proximal continental shelf geomorphology

The cartographic synthesis of the southwestern coast of Sardinia of inland and offshore areas at the scale 1:25,000 is integrated: (1) with a detailed map at 1:10,000 of the coastal area where the SOMK Mesolithic site is located and; (2) with a detailed map at 1:10,000 of the paleolandscape. The maps show the lithology from the Palaeozoic basement to the actual covers both inland and in submerged sectors. The landforms identified inland were shaped by coastal, fluvial and gravity-induced processes, and some

prolong on the seafloor. Most of submerged landforms appear to have been modeled in subaerial conditions during low stands and were sealed by the rising sea in post-glacial times.

The sandstone beachrocks at  $-45 / -50$  m correspond to those dated to the closure of the Younger Dryas in the gulf of Cagliari (Orrù et al., 2004). The intermediate platform has medium, slightly pelitic sands with a bioclastic component growing towards the lower limit of *Posidonia oceanica*. Farther offshore dominate biogenic gravels with red algae (Maerl and Pralines) form large dunes with selected grain size. The proximal platform is dominated by the bio-morphologies of the *Posidonia oceanica* on mattes prairie, articulated in deep channels iso-oriented according to the dominant bottom currents (NW). The peri-littoral sector is dominated by deposits linked to the demolition processes of the high rocky coasts. The morphology of the coastal strip is articulated by the rocky outcrops of the basement metamorphites and by the platforms of Holocene abrasion, engraved in the sandstones and coastal conglomerates of MIS 5 which extend up to an altitude of  $-4$  m, about 140 m from the edge of present cliffs. On the submerged beach and along the coast morphologies linked to a strong coastal drift current and to frequent rip-current episodes are evident.

### 4.2. Cliff stratigraphy along the coast of Portu Maga

The lithological and sedimentological characters of the succession that emerges in the cliff are summarized in Figure 3.

At the base a conglomerate with metamorphic pebbles and a fossiliferous sandstone with plane-parallel lamination leans in discordance on an irregular wave-cut platform on the metamorphic substrate (Figure 4(a)). At Piscinas, 2 km south of Portu Maga, it is dated to MIS 5 (Palmerini & Ulzega, 1969). The sequence starts with a heterometric conglomerate with large metamorphic blocks at the base (Figure 4(b)), followed by glomerates and fossiliferous sandstones with plane-parallel lamination up to +2.5 m a.s.l. including *Patella ferruginea* and *Glycymeris* sp. On this transgressive level, with high-energy sediments, rests a sequence of biogenic limestones of *Lithotamnium* recife. The Last Interglacial series closes with medium and coarse sands with slightly inclined plane-parallel lamination (Figure 4 (c,d)).

Above it, the transition to the sequence of continental deposits is on an irregular erosion platform at times mediated by a paleosol or colluvium with a strongly reddened matrix (Figure 4(e)). The series of eolian sandstones with crossed lamination is interrupted by erosion surfaces engraved by paleo-river

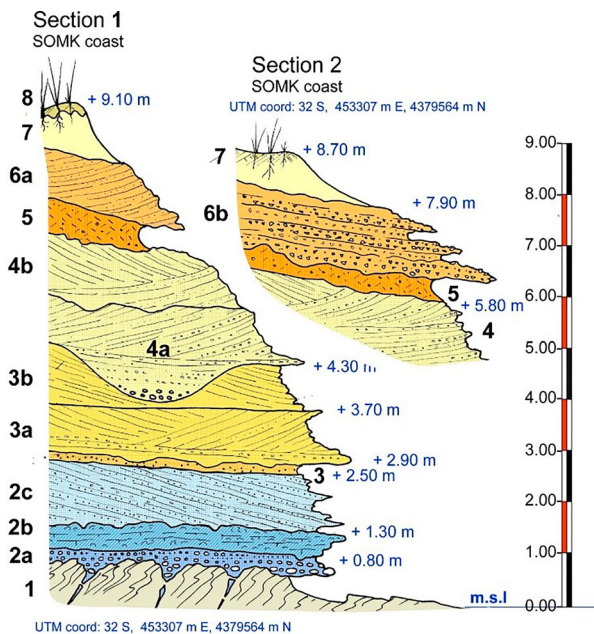


**Figure 3.** Stratigraphic sections of the Upper Pleistocene sequence of Portu Maga: (1) meta-sandstones of metamorphic substrate; (2a) polygenic heterometric conglomerate with a fossiliferous arenaceous matrix (MIS5); (2b) biogenic limestones with *Lithotamnium* (MIS5); (2c) planar-parallel lamination sandstones alternating with foreset levels (MIS5); (3) sandy palaeosol with a strongly oxidized matrix; (2f); (3a) cross-laminated eolian sandstones containing foraminifera and gastropods pulmonata *Helicidae* (MIS 4?); (4a) paleolaveo filled with sands and gravels with pulmonata gastropods (MIS 3?); (4b) cross-laminated eolian sandstones and vertebrate remains *Megaceros cazioti* (5) eolized colluvium; (6a) lightly cemented cross-laminated eolian sandstones (MIS 2); (6b) stratified slope deposit (éboulis ordonnés).



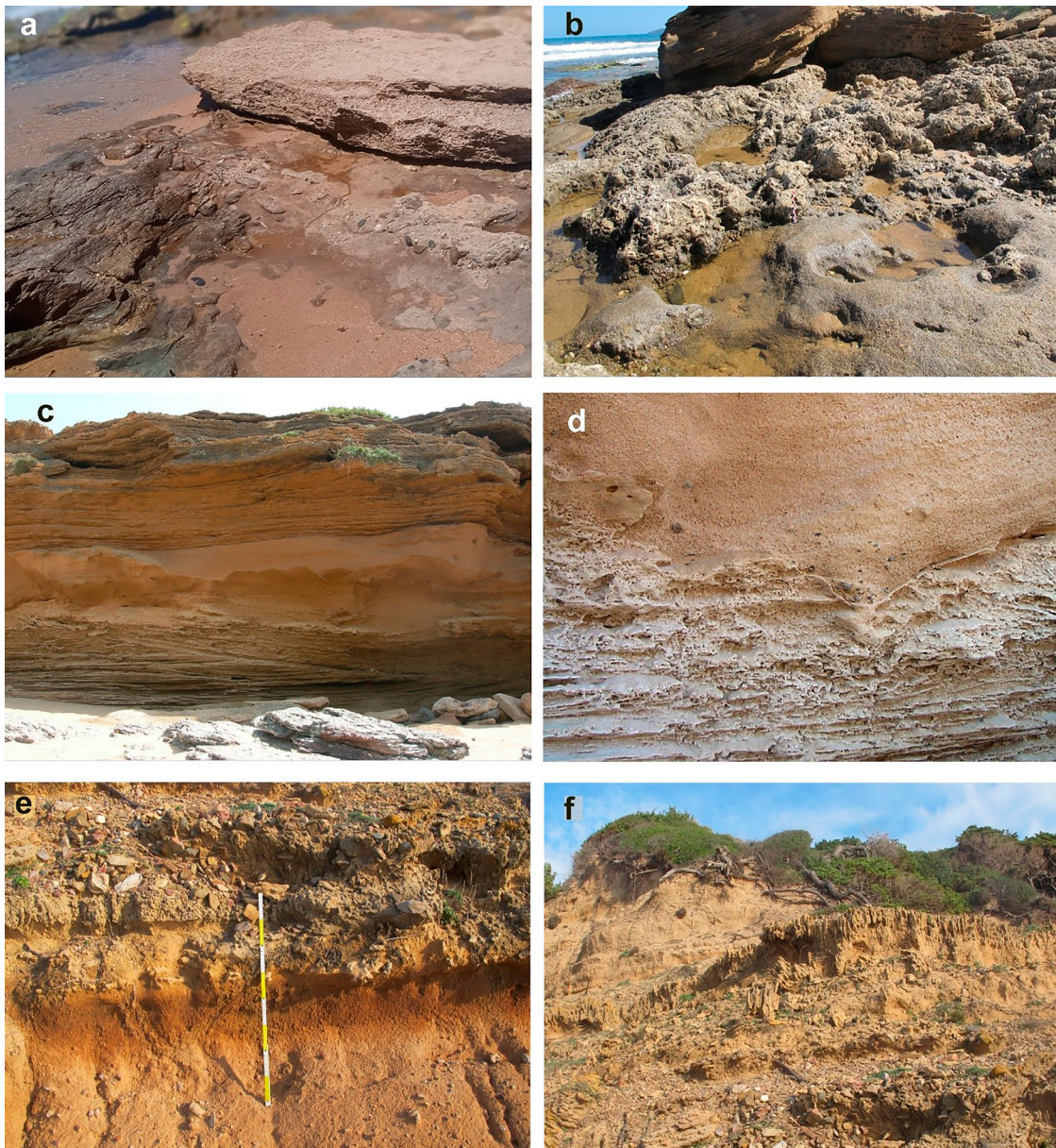


**Figure 4.** (a) a view of MIS 5 abrasion platform engraved in fossiliferous metasyllites and metargillites of the upper-middle Ordovician (Section 1). On the irregular erosional surface lay polygenic conglomerates with a fossiliferous arenaceous matrix (*Glycimeris sp.*, *Patella ferruginea*) (MIS 5.5 – Section 2a) on which an irregular level of biogenic *Lithotamnium* limestones (MIS 5.5 – Section 2b) develops, followed by medium sandstones and large quartz-feldspathic high seashores with slightly inclined plane-parallel lamination (MIS 5 – Section 2c). (b) Detail of the biogenic limestone with *Lithotamnium* passing through biocalcarenite (Section 2b); (c) Eolian cross-laminated sandstones, containing foraminifera, remains of pulmonate gastropods and vertebraries (*Prolagus s.*) (MIS 4/3 – Section 3a / 3b). (d) river paleo-incision filled by flux deposit (MIS 3? – Section 4 °). (e) paleosol with an oxidized matrix surmounted by a deposit of stratified slopes (éboulis ordonnés) (MIS 2 – Section 5 / 6b). (f) sandy paleosol with rhizoconcretions on which slope deposits and dunes rest (MIS 2/1 – Section 6a/7).

beds filled with heterometric gravels in a sandy matrix containing the remains of pulmonate gastropods. Facies analogy with sequences on the coast of the Sinis peninsula and Alghero-Argentiera, north of Portu Maga, suggests stages MIS 4/3 (Pascucci et al., 2018). The eolian deposition was interrupted by the climatic stiffening of MIS 2. Eolized colluvium is capped by stratified slope deposits in facies of *éboulis ordonnés* (LGM) (Figure 4(f)). Then, during the Holocene, fine and medium sand dunes deposited, both weakly cemented and free. The overall continental sequence is up to 10 meters thick.

### 4.3. Cliff retreating processes

The Portu Maga cliff, which is exposed to high energetic waves from NW, is currently affected by rapid retreating processes (Figure 5(a,b)). The retreat speed is linked to the lithological characteristics of the Pleistocene series, which are mainly scarcely and irregularly cemented eolian sandstones. Furthermore, weathering processes lead the evolution of differential erosion morphoscultures. Sea spray, dissolution and aolclasm are added to continental processes (rainsplash, karstism, sheetwash erosion, rilling, gullyng etc.)



At the cliff toe, which happens to be partially masked by littoral and gravitational deposits, there is a cliff base undercut linked to the expansion of the maximum breakpoints (Figure 5(c,d)).

Extreme meteorological events cause rockfalls and toppling landslides driven by preferential fracturing lines parallel to the cliff face.

Low magnitude landslides occur on a seasonal or annual basis, involving volumes of less than 10 m<sup>3</sup> with metric or sub-metric retreat niches. Major landslides, with a 5 year frequency, affect the cliff over 4/5 meters, involving hundreds of m<sup>3</sup>.

Morpho-topographic surveys were performed using multitemporal and multiscale aerial and UAV data processed through a GIS support. The analysis of the gravitational events frequency along the entire cliff point to an overall cliff retreat speed of 4 cm/y (Figure 5(e)).

The rock geomechanical parameters are linked to the waves energy that triggers deep furrows of maximum run up at the base of the cliffs. This interaction results in numerous gravitational events (rock fall and toppling).

In d is shows a 3d model of Portu Maga cliff south of the SOMK site. Storm berm from extreme waves, in metric blocks of high beach sandstone of MIS 5 (Section 2c) in imbricated position. In e is shows a 3d model of Portu Maga cliff south of the SOMK site. The model shows the comparison between DTM from aerial photographs, from drones integrated with reflex photo shoots (spring 2017, summer 2020), showing changes that occurred on the cliff surface (scale on the right is in meters).

#### 4.4. Soft rock cliff recession model

The retreat of the Portu Maga cliff due to a landslide is linked to base waveundercut processes at the base (runup notch) groove in the aeolian sandstones (*Late Pleistocene*), characterized by compressive strength of 18 Mpa and specific weight of 1.9 g/cm<sup>3</sup>.

Great attention has been paid to improve the model of the physic characteristics of the impact pressures due to breaking waves on a vertical cliff. Specifically,  $A$  was calculated as the product of three factors ( $A_i$ ) representing:

- The wave asymmetry and skewness in the pressure diagram ( $A_1$ );
- The impulsive breaking wave pressure (Goda, 2010) ( $A_2$ );
- The relations between representative wave heights ( $A_3$ ).

$$A = \prod_{i=1}^3 A_i \quad (3)$$

The numerical analysis allows to determine the cliff recession speed. The following parameters were used for the cliff of Portu Maga (Table 1):  $\sigma_c$  was estimated for eolian sandstones with weak calcite cementation (Upper Pleistocene) (specific weight:  $\gamma_g = 1900 \text{ Kg/m}^3$ ).

The model was applied with a confidence interval of 95% ( $\Delta_{95}$ ) to estimate from EWA the wave return period at 10 m depth, with  $F_w > F_R$  and erosion occurring at the cliff toe. The 5-year wave height was therefore selected as the one whose properties could define the conditions of potential collapse due to overturning of the rock mass under an assigned level of uncertainty (Table 2).

Results are compatible with geomorphological data on cliff retreat process, which, by considering a return period of 5 years, produces over 20 successive events an average retreat of the entire cliff of about 4 m in 100 years (i.e. with a retreat rate 4 cm/y).

#### 4.5. Site stratigraphy and chronology

The SOMK stratigraphy consists of sandy to coarse deposits with interbedded archaeological remains in a rockshelter which evolved in the eolianites (Figure 6(a,b)) (Cristiani et al., 2021; Floris et al., 2012; Melis et al., 2012; Melis & Mussi, 2016). Multiple 14C dates bracket the deposition between ca 9000 and 8000 yr cal BP (Table 3).

At the bottom, on the eolianite, a massive reddish sand eolian deposit is covered by dark gray debris and sands up to ~0.3 m-thick with dispersed obsidian and jasper artifacts, human bone fragments, abundant *Prolagus sardus* (an endemic fairly-sized micromammal), charcoal and ashes. It is dated to ca 9212 ± 91 yr cal BP (Table 3). Near the cliff wall, a partial adult skeleton was discovered (SOMK3) (Figure 6 (c)) (Melis and Mussi 2016) capped by a chaotic deposit (about 1 m thick) with massive structures and debris of different shapes and sizes in a gray sandy silt matrix. At the bottom there are rounded metamorphic and eolianite pebbles and boulders up to 30 cm-long. Boulders are also found grouped near the eolianite wall next to SOMK3 (Figure 6(a)). The coarse sediments are mainly directed from southeast to northwest. In the matrix there are dispersed obsidian and jasper artifacts as well as abundant *Prolagus sardus* and *Tyrrenicola henseli*, another endemic micromammal.

The characteristics of this deposit suggest an alluvial episode such as a debris flow or gravity flow from the rear slope. Next, another debris flow deposited. It is massive and chaotic, with dominant metamorphic rounded cobbles in a dark gray detrital sandy matrix which is extremely rich in ash. The cobbles ( $\geq 10 \text{ cm}$ ) are mainly northwest-oriented. In the matrix, there is abundant *Prolagus sardus* and



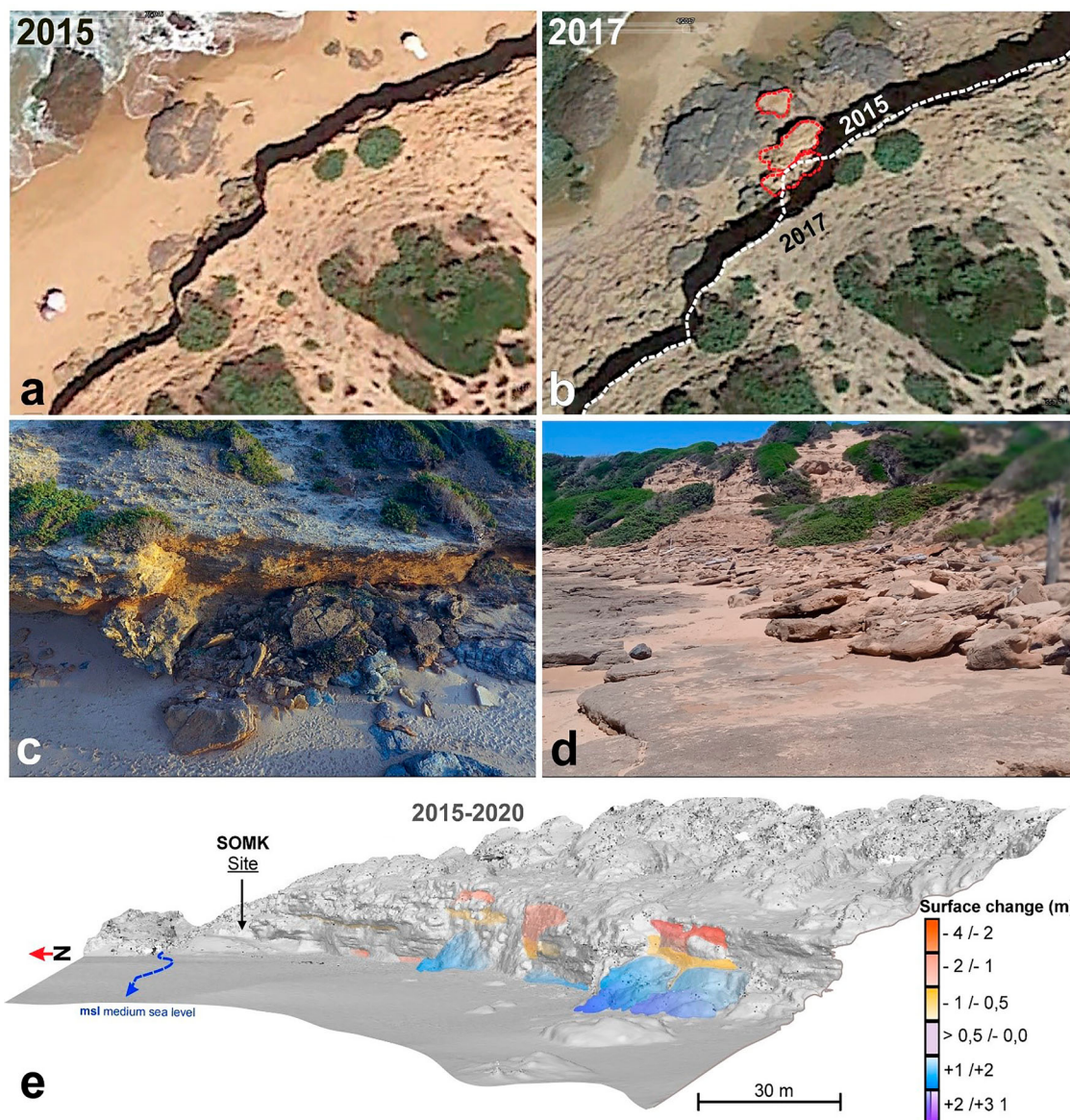


**Figure 5.** (a) Edge of the cliff of Portu Maga, comparison between the aerial photo of March 2015 and July 2017. (b) Particularly evident is the large landslide overturning that led to the retreat of 4 m for a stretch of 6 m mobilizing about 200 m<sup>3</sup> of materials; in the following years, the collapsed blocks were partially demolished by the action of the wave motion. (c) detail of the overturning landslide of photoaerea a and b, evident the sub-vertical planar detachment surface that documents the structural control along the fracture. (d) Portu Maga cliff south of the SOMK site. Storm berm from extreme waves, in metric blocks of high beach sandstone of MIS 5 (Section 2c) in imbricated position. (e) Portu Maga cliff south of the SOMK site. Model 3 D comparison between reliefs from aerial photographs, from drones integrated with reflex photo shoots (spring 2017, summer 2020), showing changes that occurred on the cliff surface (scale on the right is in meters).

*Tyrrenicola henseli* with scattered obsidian and jasper artifacts. Two more partial skeletons, SOMK1 (Figure 6(d)) and SOMK2, were found lying at the top of this deposit. A rockfall, about 150 cm-thick, with eolianite blocks covers the sequence and the skeletons. In turn it is overlain by a compact sandy eolian and colluvial deposit with eolianite debris. The sequence ends with recent aeolian deposits.

**Table 1.** Model parameter values at Portu Maga cliff.

$\sigma_c$ [Mpa]	RMi [Mpa]	$A_1$	$A_2$	$A_3$
18	3.2	1.5	9	2

## 5. Discussion

### 5.1. Evolution of the cliff/platform

The accelerated retreat of the Portu Maga cliff and SOMK site is the outcome of rapidly evolving rockfalls and toppling. The geomorphological survey shows that the main gravitational events cyclically happen every 5 years. Furthermore, the landslide deposits

**Table 2.** 5-year wave height in a 95% confidence interval and associated force from the proposed model.

$T_r$ [year]	$H_5 + \Delta_{95}$ [m]	$F_w$ [Mpa]
5	10.2	3.3



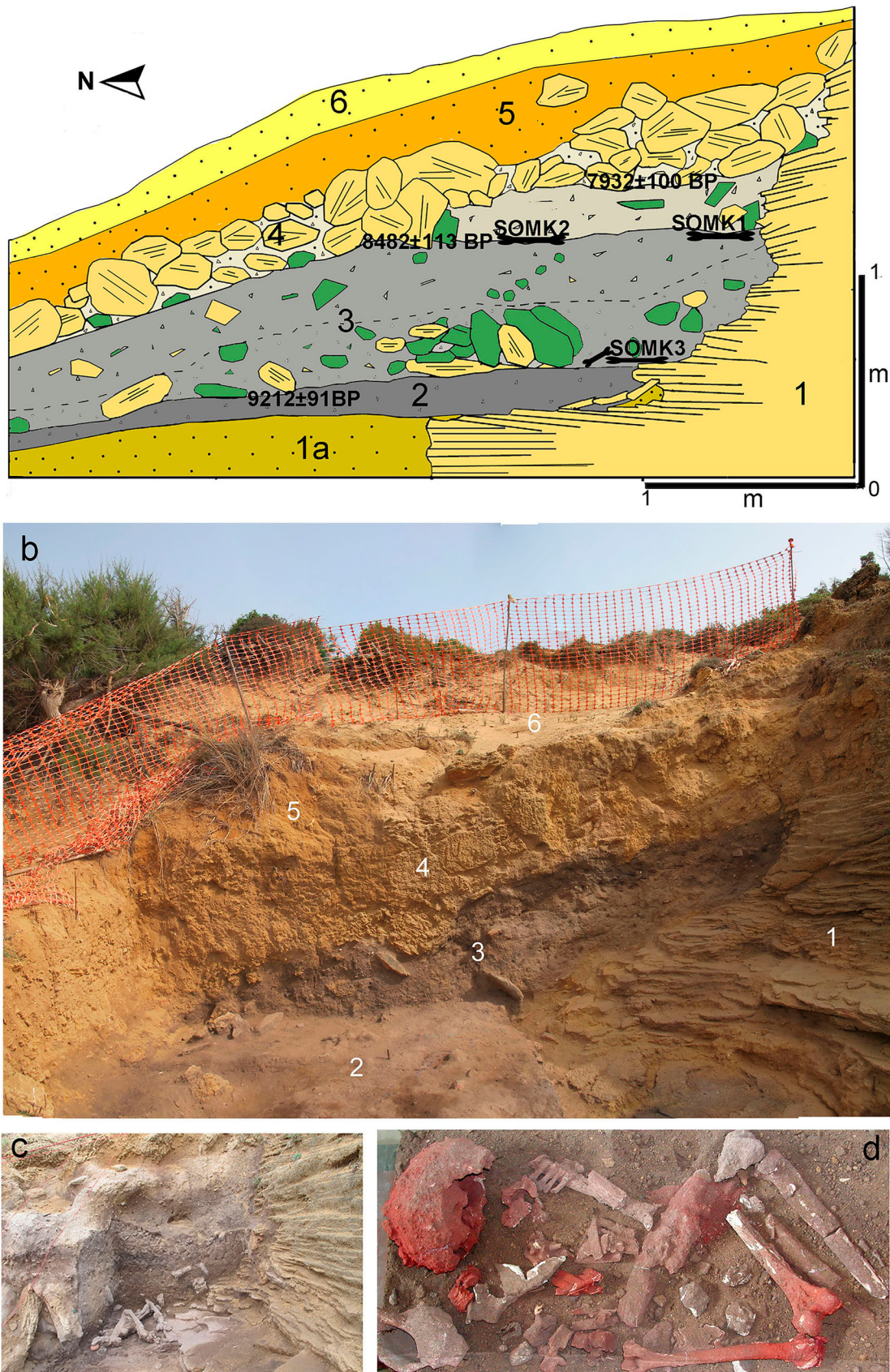


**Figure 6.** SOMK site. (a) schematic lithostratigraphic section: (1) Pleistocene eolianite; (1a) eolian sand deposits on the eolianite; (2) anthropic level with hearths; (3) debris flow deposits with ash; (4) rockfall deposit; (5) massive sandy eolian and colluvial deposit with eolianite debris; (6) recent eolian deposits; (b) view of the site lithostratigraphy: (1) Pleistocene eolianite; (2) anthropic level with hearths; (3) debris flow deposits with ash; (4) rockfall deposit; (5) massive sandy eolian and colluvial deposit with eolianite debris; (6) recent eolian deposits; (c) skeletal remains (SOMK 3) covered by the debris flow deposits (after Melis & Mussi, 2016); (d) heavily ochre-stained skeletal remains (SOMK 1) at the top of debris flow deposits (after Melis & Mussi, 2016).



**Table 3.** Radiocarbon dating results. The calibration program used is CALIB Radiocarbon Calibration Version 8.2 html (Stuiver and al., 1993) Radiocarbon dating was made in the NSF Tucson Arizona (\*) and INNOVA laboratory (Caserta) (\*\*).

Lab. ID	Sample	Sample material	$^{14}\text{C}$ age BP	$\delta^{13}\text{C}\text{‰}$	Calibration dataset	Calibrate age year BP ( $2\sigma$ ) and probability
AA79862*	I	Charcoal	$7127 \pm 59$	-24.8	IntCal20	$7932 \pm 100$ 0.99%
AA76545*	II	Human bone (SOMK2)	$7678 \pm 73$	-20.2	IntCal20	$8482 \pm 113$ 100%
AA76546*	III	Charcoal	$7860 \pm 44$	-23.5	IntCal20	$8661 \pm 119$ 0.92%
DSH9497_CH**	IV	Charcoal	$8238 \pm 24$	-27	IntCal20	$9212 \pm 91$ 0.92%
DSH7896_CH**	V	Charcoal	$8130 \pm 53$	-46	IntCal20	$9137 \pm 143$ 0.99%

are rapidly disintegrated by the wave motion energy, exposing the cliff toe and creating the wave base undercut which will lead to a new collapse.

These are large landslides that involve 4 m of retreat for each event and a width of 5/6 m depending on the mesoscale joints that determine the size of the blocks. Considering the c. 100 meter-long cliff stretch studied here in detail, after 20 events the entire cliff retreated by 4 m. In terms of time, it takes 100 years. So an average retraction speed is within 4–6 cm/y range.

The Holocene abrasion platform engraved in the sandstones and conglomerates records the maximum exposure of the Pleistocene eolianites. It reaches -4 m depth u.s.l. extending up to 140 m from the

cliff face. Considering the eustatic curve by Lambeck et al., (2011, 2014) it corresponds to the paleo shoreline of 4-3500 yr cal BP, i.e. to the Bronze Age (Depalmas & Melis, 2010).

Applying the retraction speed of 4 cm / y to this paleo shoreline of 3500 yr cal ago, we get a total set-back of about 140 meters (Figure 7). The geomorphological evidence of multi-events landslide supports the numerical analysis.

The cliff retreat reached the SOMK site exposing seawards the stratigraphic sequence. At the time of the Mesolithic settlement the entrance rather faced north towards the river as evidenced by the geo-archaeological and geomorphological study of the site and the area at large.

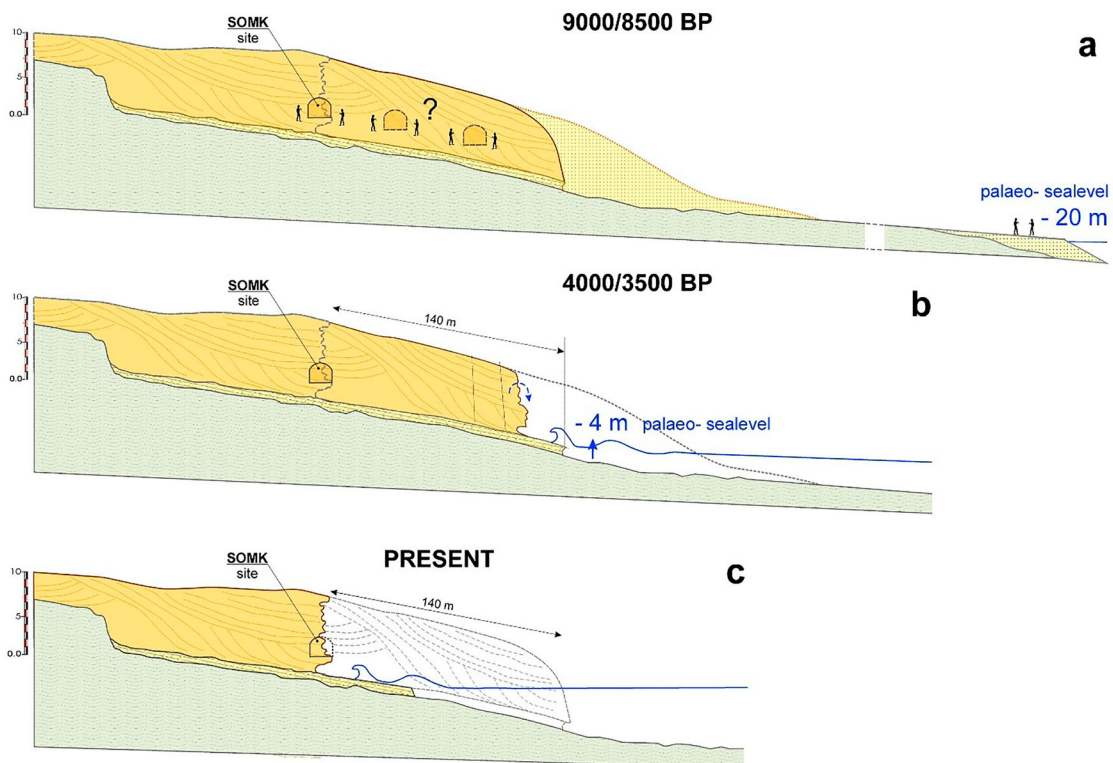


**Figure 7.** Portu Maga cliff evolutionary phases: (a) Mesolithic Age (9/8,5 Ky cal BP) palaeo sea level at -20 m, SOMK site and probable other rock shelters along the river about 1.5 km away from the shoreline. The cliff fossilized by the rampant dune; (b) Bronze Age (4/3,5 Ky cal BP), paleo-marine level at -4 m, wave energy removes dune deposits and carves the cliff in wind sandstone triggering the retreat due landslides; (c) current situation of Portu Maga following the cliff retreat estimated between 140 and 160 m.

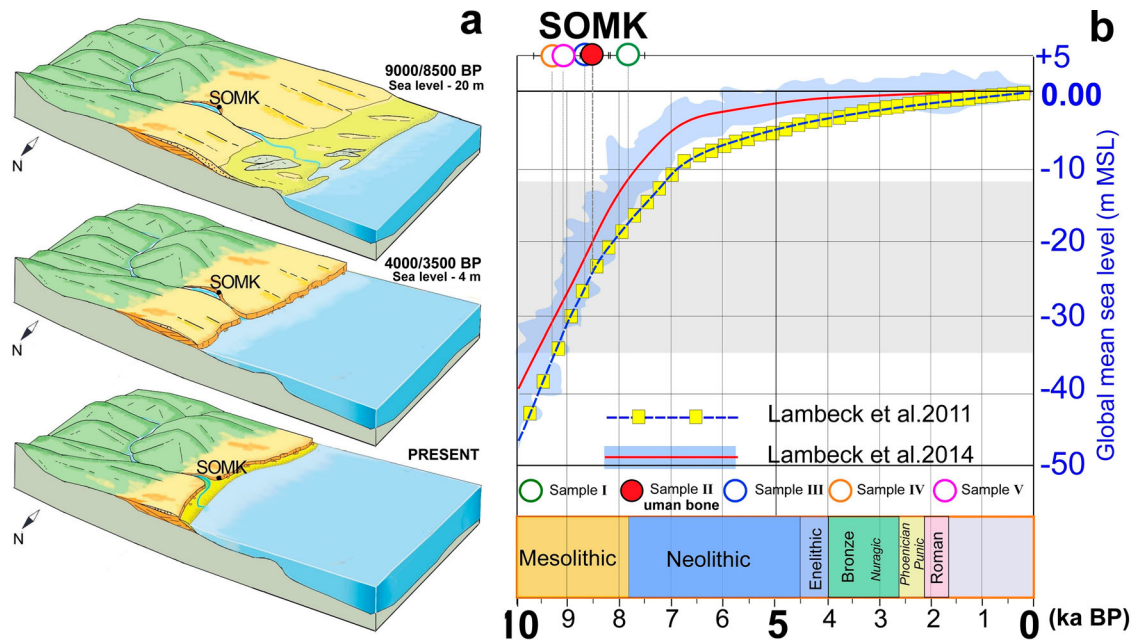


**Figure 8.** (a) Coastal landscape changes due to sea-level rise, eolian deposits, and river erosion; (b) Calibrated Ages from the SOMK samples (Table 3) plotted on the Relative sea-level prediction after Lambeck et al., 2011 and Lambeck et al., 2014, for South-wester Sardinian continental shelf.

## 5.2. Landscape and site evolution

The SOMK stratigraphic sequence reflects the complex processes affecting the area during the Early Holocene. They are the outcome of fluvial dynamics and of eolian, gravitational, and anthropic processes.

When the sea level was lower but steep cliffs had not yet formed along the coastline, some small cavities could have developed where the dunes did not completely blanket the eolianites. More could have formed on the slopes of the S'Orku e S'Orku valley, close to the river mouth, even if SOMK is the only surviving one.

After a stable period when humans periodically came to the shelter, slope and alluvial deposits impacted the site, probably as a result of a marked paleoenvironmental and climate change. Through sedimentological analyses we characterize them as a debris flows. The abundant ash in the matrix is consistent with wildfire(s) on the slope behind (e.g. Bodí et al., 2014; Carabella et al., 2019; DiBiase & Lamb, 2020). Our results support the hypothesis that they originated on the SW slope. Nowadays the original entrance of the rockshelter is completely hidden by recent eolian sediments and by eolianite rockfall. However, the direction of the coarse sediments towards the sea show that the shelter opening once was towards the valley of Rio S'Orku e S'Orku. Seaward, the exposure of the stratigraphic sequence points to a cliff retreat that led to partial site destruction. The erosional processes destroyed other cavities that we hypothesize along the coast and the river valley (Figure 8).

## 6. Conclusion

The coastal evolution of the study area is characterized by the rapid retreating processes of the high coast due to lightly cemented lithotypes, intense linear erosion by watercourses, debris flows, rockfalls, and toppling. These processes and the sea level rise canceled any evidence of Mesolithic settlements. The exceptional preservation of the collapsed SOMK rockshelter is due to a more protected morphological position and to the distance from the Early Holocene coastline.

Overall, the lack of underwater archaeology does not allow us to make hypothesis on how ancient human groups reacted when the sea level rose and impacted the late Pleistocene and Early Holocene landscapes.

The proposed approach improves the Sunamura's analytical model including some properties of wave energy and soft rock cliff. The high waves energy and the modest geo-mechanical resistance of the lithotypes led to a retreat rate of 4 cm per year at Portu Maga. Based on this result, The SOMK shelter can therefore be considered as a residual element of a much larger settlement which developed mainly along the river while the processes of retreat due to landslides represented a limiting factor for the attendance of the seafront.

The geomorphological survey of the continental shelf has made it possible to reconstruct the characteristics of the Mesolithic palaeolandscape, where the man of SOMK could frequent a sheltered coastal plain in front crossed by a stream that flowed into a large lagoon, dune fields occupied part of the plain, while rampant dunes leaned against the reliefs.



## Software

The map was digitized using ESRI ArcGIS®10.6 software. UAV photogrammetry data were processed by Agisoft Metashape Professional®. The digital terrain models were generated using the Global Mapper® 21.0.

## Open Scholarship



This article has earned the [Center for Open Science](#) badge for Open Materials. The materials are openly accessible at .

## Acknowledgements

We are grateful to Gruppo Archeologico Neapolis (Guspini) and Comune di Arbus for the continuous support. The research permits were received through Soprintendenza Archeologica di Cagliari. The research was supported by Università di Cagliari (FDS 2020- CAR 2019) and Parco Geominerario (2019).



## Disclosure statement

No potential conflict of interest was reported by the author(s).

## ORCID

Rita Teresa Melis  <http://orcid.org/0000-0003-1095-8696>  
Valentino Demurtas  <http://orcid.org/0000-0003-4187-0902>

Margherita Mussi  <http://orcid.org/0000-0001-9393-9591>  
Paolo Emanuele Orrù  <http://orcid.org/0000-0002-2394-3154>

Flavio Altamura  <http://orcid.org/0000-0001-6074-5213>  
Giacomo Deiana  <http://orcid.org/0000-0002-7019-9153>

## Data availability statement

Raw data were generated at University of Cagliari (Italy). Derived data supporting the findings of this study are available on request from the corresponding author.

## References

- Ammerman, A. J. (2020). Cyprus: The submerged final palaeolithic of aspros dive site C. In G. Bailey, N. Galanidou, H. Peeters, H. Jöns, & M. Mennenga (Eds.), *The archaeology of Europe's drowned landscapes. Coastal research library*, (Vol. 35, pp. 429–442). Springer.
- Andreucci, S., Clemmensen, L. B., Murray, A. S., & Pascucci, V. (2010). Middle to late Pleistocene coastal deposits of Alghero, northwest Sardinia (Italy): chronology and evolution. *Quaternary International*, 222(1-2), 3–16. <https://doi.org/10.1016/j.quaint.2009.07.025>
- Bailey, G., & Cawthra, H. (2021). The significance of sea-level change and ancient submerged landscapes in human dispersal and development: A geoarchaeological perspective. *Oceanologia*, 1–21. ISSN 0078-3234, <https://doi.org/10.1016/j.oceano.2021.10.002>
- Bailey, G. N., & Flemming N. C. (2008). Archaeology of the continental shelf: Marine resources, submerged landscapes and underwater archaeology. *Science Reviews*, 27 (23–24), 2153–2165. <https://doi.org/10.1016/j.quascirev.2008.08.012>
- Benjamin, J., Rovere, A., Fontana, A., Furlani, S., Vacchi, M., Inglis, R. H., Galili, E., Antonioli, F., Sivan, D., Miko, S., Mourtzas, N., Felja, I., Meredith-Williams, M., Goodman-Tchernov, B., Kolaiti, E., Anzidei, M., & Gehrels, R. (2017). Late quaternary sea-level changes and early human societies in the central and eastern Mediterranean basin: An interdisciplinary review. *Quaternary International*, 449, 29–57. <https://doi.org/10.1016/j.quaint.2017.06.025>
- Bodí, M. B., Martin, D. A., Balfou, r. V. N., Santín, C., Doerr, S. H., Pereira, P., Cerdà, A., & Mataix-Solera, J. (2014). Wildland fire ash: Production, composition, and eco-hydro-geomorphic effects. *Earth-Science Reviews*, 130 (2014), 103–127. <https://doi.org/10.1016/j.earscirev.2013.12.007>
- Brooks, S. M., Spencer, T., & Boreham, S. (2012). Deriving mechanisms and thresholds for cliff retreat in soft-rock cliffs under changing climates: Rapidly retreating cliffs of the Suffolk coast, UK. *Geomorphology*, 153-154, 48–60. <https://doi.org/10.1016/j.geomorph.2012.02.007>
- Budetta, P., Galiotta, G., & Santo, A. (2000). A methodology for the study of the relation between coastal cliff erosion and the mechanical strength of soils and rock masses. *Engineering Geology*, 56(56), 243–256. [https://doi.org/10.1016/S0013-7952\(99\)00089-7](https://doi.org/10.1016/S0013-7952(99)00089-7)
- Carabella, C., Miccadei, E., Paglia, G., & Sciarra, N. (2019). Post-wildfire landslide hazard assessment: The case of The 2017 Montagna Del Morrone fire (central Apennines, Italy) reflected in the spatial coverage of ash, but also in the range of the ash color. Wildland fire ash: Production, composition and eco-hydro-geomorphic effects. *Geosciences*, 9(9), 175. <https://doi.org/10.3390/geosciences9040175>
- Carmignani, L., Oggiano, G., Funedda, A., Conti, P., & Pasci, S. (2015). The geological map of sardinia (Italy) at 1: 250,000 scale. *Journal of Maps*, 12(5), 826–835. <http://doi.org/10.1080/17445647.2015.1084544>.
- Castagnino Berlinghieri, E. F., Antonioli, F., & Bailey, G. (2020). Italy: The archaeology of palaeoshorelines, coastal caves and seafaring connections. In G. Bailey, N. Galanidou, H. Peeters, H. Jöns, & M. Mennenga (Eds.), *The archaeology of Europe's drowned landscapes. Coastal research library*, 35 (pp. 321–340). Springer. [https://doi.org/10.1007/978-3-030-37367-2\\_16](https://doi.org/10.1007/978-3-030-37367-2_16)
- Castedo, R., Murphy, W., Lawrence, J., & Paredes, C. (2012). A new process–response coast-al recession model of soft rock cliffs. *Geomorphology*, 177–178, 128–143. <https://doi.org/10.1016/j.geomorph.2012.07.020>
- Chelli, A., Aringoli, D., Aucelli, P. P. C., Baldassarre, M. A., Bellotti, P., Bini, M., Biolchi, S., Bontempi, s., Brandolini, P., Davoli, L., Deiana, G., & Valente, A. (2018). Morphodynamics of coastal areas represented in the new geomorphologic map of Italy: Draw the landforms of the past to outline the future. *Alpine and Mediterranean Quaternary*, 31(1), 17–21. <http://amq.aiqua.it/index.php/issues-2012-2017/alpine-and-mediterranean-quaternary-vol-31-1-quaternary-past-presentfuture-aiqua-conference-florence-13-14-06-2018/959>

- Cristiani, E., Melis, R. T., & Mussi, M. (2021). *Marine shells as grave goods at S'Ormu e S'Orku (Sardinia, Italy)*. FORAGING assemblages Conference. Vol. 2 / edited by Dušan Borić, Dragana Antonović, and Bojana Mihailović. - Belgrade: Serbian Archaeological Society; New York: The Italian Academy for Advanced Studies in America, Columbia University, 2021 (Belgrade: Publikum). - VIII str., str. 353-820.
- Deiana, G., Antonioli, F., Moretti, L., Orrù, P. E., Randazzo, G., & Lo Presti, V. (2021). MIS 5.5 highstand and future sea level flooding at 2100 and 2300 in tectonically stable areas of central Mediterranean sea: Sardinia and the pontina plain (Southern Latium), Italy. *Water (Switzerland)*, 13(18), 2597. <https://doi.org/10.3390/w13182597>
- Deiana, G., Lecca, L., Melis, R. T., Soldati, M., Demurtas, V., & Orrù, P. E. (2021). Submarine geomorphology of the southwestern sardinian continental shelf (Mediterranean sea): insights into the last glacial maximum sea-level changes and related environments. *Water (Switzerland)*, 13(2). <https://doi.org/10.3390/w13020155>.
- Deiana, G., Orrù, P. E., & Demurtas, V. (2022). Bedforms of Bonifacio Strait (western Mediterranean): hydrodynamics, coastal outline, supply and sediment distribution. *Geological Society, London, Special Publications*, 523. <https://doi.org/10.1144/SP523-2022-10>
- Del Río, L., & Gracia, F. J. (2009). Erosion risk assessment of active coastal cliffs in temperate environments. *Geomorphology*, 112(1-2), 82–95. <https://doi.org/10.1016/j.geomorph.2009.05.009>
- Del Río, L., Posanski, D., Gracia, J., & Pérez-Romero, A. M. (2020). A comparative approach of monitoring techniques to assess erosion processes on soft cliffs. *Bulletin of Engineering Geology and the Environment*, 79(4), 1797–1814. <https://doi.org/10.1007/s10064-019-01680-2>
- Demurtas, V., Orrù, P. E., & Deiana, G. (2021a). Evolution of deep-seated gravitational slope deformations in relation with uplift and fluvial capture processes in central eastern sardinia (Italy). *Land*, 10(11), 1193. <https://doi.org/10.3390/land10111193>
- Demurtas, V., Orrù, P. E., & Deiana, G. (2021b). Deep-seated gravitational slope deformations in central sardinia: Insights into the geomorphological evolution. *Journal of Maps*, 17(2), 594–607. <https://doi.org/10.1080/17445647.2021.1986157>
- Depalmas, A., & Melis, R. T. (2010). The nuragic people: Their settlements, economic activities and use of the land. In P. I. Martini & W. Chesworth (Eds.), *Landscapes and societies. Selected cases* (pp. 167–186). Springer.
- DiBiase, R. A., & Lamb, M. P. (2020). Dry sediment loading of headwater channels fuels post-wildfire debris flows in bedrock landscapes. *Geology*, 48(2), 189–193. <https://doi.org/10.1130/G46847.1>
- Duguet, T., Duperré, A., Costa, S., Regard, V., & Maillet, G. (2021). Coastal chalk cliff retreat rates during the Holocene, inferred from submarine platform morphology and cosmogenic exposure along the normandy coast (NW France). *Marine Geology*, 433(2021), 106405. <https://doi.org/10.1016/j.margeo.2020.106405>
- Ferranti, L., Antonioli, F., Mauz, B., Amorosi, A., Dai Pra, G., Mastronuzzi, G., Monaco, C., Orrù, P., Pappalardo, M., Radtke, U., Renda, P., Romano, P., Sansò, P., & Verrubbi, V. (2006). Markers of the last interglacial sea-level high stand along the coast of Italy: Tectonic implications. *Quaternary International*, 145, 30–54. <https://doi.org/10.1016/j.quaint.2005.07.009>
- Floris, R., Melis, R. T., Mussi, M., Palombo, M. R., Iacumin, P., Usai, A., & Mascia, A. (2012). La presenza umana nella Sardegna, centro occidentale durante l'Olocene antico: Il sito di S'Ormu e S'Orku (Arbus, VS). Il Mesolitico della Sardegna nel contesto insulare tirrenico. In *Atti della XLIV Riunione Scientifica dell'Istituto Italiano di Preistoria e Protostoria: La Preistoria e la Protostoria della Sardegna*: Cagliari, Barumini, Sassari 23–28 novembre 2009, 999–1004. Firenze, Istituto Italiano di Preistoria e Protostoria.
- Furlani, S., Pappalardo, M., Gomez-Pujol, L., & Chelli, A. (2014). The rock coast of the Mediterranean and black seas. In D. M. Kennedy, W. J. Stephenson, & L. Naylor (Eds.), *Rock coast geomorphology: A global synthesis* (Vol. 40, pp. 89–122). Avon: Geological Society Memoirs, published by Geological Society Publishing House
- Galanidou, N., & Bailey, G. (2020). The Mediterranean and the Black Sea: Introduction. In G. Bailey, N. Galanidou, H. Peeters, H. Jöns, & M. Mennenga (Eds.), *The archaeology of Europe's drowned landscapes. Coastal research library*, vol 35, 309–319. Springer.
- Galanidou, N., Dellaporta, K., & Sakellariou, D. (2020). Greece: Unstable landscapes and underwater archaeology. In G. Bailey, N. Galanidou, H. Peeters, H. Jöns, & M. Mennenga (Eds.), *The archaeology of Europe's drowned landscapes. Coastal research library*, vol 35, (pp. 371–392). Springer. [https://doi.org/10.1007/978-3-030-37367-2\\_16](https://doi.org/10.1007/978-3-030-37367-2_16).
- Gallili, E., Rosen, B., Weinstein Evron, M., Hershkovitz, I., Es-hed, V., & Horwitz, L. K. (2020). Israel: Submerged prehistoric sites and settlements on the Mediterranean coastline—the current state of the art. In G. Bailey, N. Galanidou, H. Peeters, H. Jöns, & M. Mennenga (Eds.), *The archaeology of Europe's drowned landscapes* (pp. 443–481). Springer. [https://doi.org/10.1007/978-3-030-37367-2\\_23](https://doi.org/10.1007/978-3-030-37367-2_23).
- Gambin, T. (2020). Malta: Submerged landscapes and early navigation. In G. Bailey, N. Galanidou, H. Peeters, H. Jöns, & M. Mennenga (Eds.), *The archaeology of Europe's drowned landscapes. Coastal research library*, vol 35 (pp. 341–346). Springer. [https://doi.org/10.1007/978-3-030-37367-2\\_16](https://doi.org/10.1007/978-3-030-37367-2_16).
- Geoff, B., Søren, A. H., & Thijs, J. M. (2020). Denmark: Mesolithic coastal landscapes submerged. *The Archaeology of Europe's Drowned Landscapes*, 35. [https://dx.doi.org/10.1007/978-3-030-37367-2\\_3](https://dx.doi.org/10.1007/978-3-030-37367-2_3).
- Goda, Y. (2010). *Random seas and design of maritime structures* (3rd ed, p. 732). World Scientific.
- Lambeck, K., Antonioli, F., Anzidei, M., Ferranti, L., Leoni, G., Scicchitano, G., & Silenzi, S. (2011). Sea level change along Italian coast during Holocene and a projection for the future. *Quaternary International*, 2011(232), 250–257. <https://doi.org/10.1016/j.quaint.2010.04.026>
- Lambeck, K., Rouby, H., Purcell, A., Sun, Y., & Sambridge, M. (2014). Sea level and global ice volumes from the last glacial maximum to the Holocene. *Proceedings of the National Academy of Sciences of the USA*, 111(43), 15296–15303. <https://doi.org/10.1073/pnas.1411762111>
- Martini, F., & Tozzi, C. (2012). *Il Mesolitico in Sardegna*. Atti della XLIV Riunione Scientifica dell'I.I.P.P. “La Preistoria e la Protostoria della Sardegna”, 23-28 novembre 2009, vol. I, 399–406.
- Melis, R. T., & Mussi, M. (2016). Mesolithic burials at S'Ormu e S'Orku (SOMK) on the south-western coast of sardinia. In J. M. Grunberg, B. Gramsch, L. Larsson, J. Orschiedt, & H. Meller (Eds.), *Mesolithic burials –*



- rites, symbols and social organisation of early postglacial communities (pp. 733–740), *International Conference Halle (Saale), Germany, 18th–21st September 2013* (Tagungen des Landesmuseums für Vorgeschichte Halle 13/II). Halle (Saale), Landesamt für Denkmalpflege und Archäologie Sachsen-Anhalt, Landesmuseum für Vorgeschichte.
- Melis, R. T., Mussi, M., Floris, R., Lamothe, M., Palombo, M. R., & Usai, A. (2012). *Popolamento e ambiente nella Sardegna centro occidentale durante l'Olocene antico: primi risultati*. Atti della XLIV Riunione Scientifica dell'Istituto Italiano di Preistoria e Protostoria: La Preistoria e la Protostoria della Sardegna: Cagliari, Barumini, Sassari 23–28 novembre 2009, 427–34. Firenze.
- Muñoz Narciso, E., García, H., Sierra Pernas, C., & Pérez-Alberti, A. (2017). Study of geomorphological changes by high quality DEMs, obtained from UAVs—structure from motion in highest continental cliffs of Europe: A Capelada (Galicia, Spain). *Geophys Res Abstr EGU Gen Assem*, 19, 2017–2692.
- Orrù, P., Solinas, E., Puliga, G., & Deiana, G. (2011). Palaeo-shorelines of the historic period. Sant'Antioco Island, south-western Sardinia (Italy). *Quaternary International*, 232(1–2), 71–81. <https://doi.org/10.1016/j.quaint.2010.06.004>
- Orrù, P. E., Antonioli, F., Lambeck, K., & Verrubbi, V. (2004). Holocene sea-level change in the Cagliari coastal plain (South Sardinia, Italy). *Quaternaria Nova*, VIII, 193–210. Roma.
- Orru, P. E., Deiana, G., Taviani, M., & Todde, S. (2012). Palaeoenvironmental reconstruction of the last glacial maximum coastline on the San Pietro continental shelf (Sardinia SW). *Rendiconti Online Società Geologica Italiana*, 21(2), 1182–1184.
- Orrù, P. E., Mastronuzzi, G., Deiana, G., Pignatelli, C., Piscitelli, A., Solinas, E., Spanu P. G., & Zucca R. (2014). Sea level changes and geoarchaeology between the Bay of Capo Malfatano and Piscinni Bay (SW Sardinia) in the last 4 Kys. *Quaternary International*, 336, 180–189. <https://doi.org/10.1016/j.quaint.2014.03.054>
- Palmerini, V., & Ulzega, A. (1969). Sedimentologia e geomorfologia del settore costiero tra la foce del Rio Piscinas e Capo Pecora. *Seminario della Facoltà di Scienze dell'Università di Cagliari*, 34, 1–38.
- Palmstrøm, A. (1996). Characterizing rock masses by the RMI for use in practical rock engineering: Part 1: The development of the rock mass index (RMI). *Tunnelling and Underground Space Technology*, 11(2), 175–188. [https://doi.org/10.1016/0886-7798\(96\)00015-6](https://doi.org/10.1016/0886-7798(96)00015-6)
- Palombo, M. R., Antonioli, F., Lo Presti, V., Mannino, M. A., Melis, R. T., Orru, P., Stocchi, P., Talamo, S., Quarta, G., Calcagnile, L., Deiana, G., & Altamura, S. (2017). The late Pleistocene to Holocene palaeogeographic evolution of the Porto Conte area: Clues for a better understanding of human colonization of sardinia and faunal dynamics during the last 30 ka. *Quaternary International*, 2017(439), 117–140. <https://doi.org/10.1016/j.quaint.2016.06.014>
- Pascucci, V., Andreucci, S., Sechi, D., & Casini, L. (2018). Late quaternary stratigraphy of western sardinia (central Mediterranean) based on luminescence age dating. *Alpine and Mediterranean Quaternary*, 31(1), 181–184.
- Putignano, M. L., Orrù, P. E., & Schiattarella, M. (2014). Holocene coastline evolution of Procida Island, Bay of Naples, Italy. *Quaternary International*, 332, 115–125. <https://doi.org/10.1016/j.quaint.2014.03.003>
- Radić Rossi, I., Karavanić, I., & Butorac, V. (2020). In G. Bailey, N. Galanidou, H. Peeters, H. Jöns, & M. Mennenga (Eds.), *The archaeology of Europe's drowned landscapes*. Coastal Research Library, 35, 347–369. Springer, Cham. [https://doi.org/10.1007/978-3-030-37367-2\\_16](https://doi.org/10.1007/978-3-030-37367-2_16).
- Skaarup, J., & Grøn, O. (2004). *Møllegabet II. A submerged mesolithic settlement in southern Denmark*. BAR Int. Ser. 1328 Archaeo- press, Oxford.
- Stuiver, M., & Reimer, P. J. (1993). *Radiocarbon*, 35(1), 215–230.
- Sulis, A., & Annis, A. (2014). Morphological response of a sandy shoreline to a natural obstacle at Sa Mesa Longa Beach, Italy. *Coastal Engineering*, 2014(84), 10–22. <https://doi.org/10.1016/j.coastaleng.2013.10.014>
- Sulis, A., Cozza, R., & Annis, A. (2017). Extreme wave analysis methods in the gulf of Cagliari (South Sardinia, Italy). *Ocean & Coastal Management*, 140, 79–87. <https://doi.org/10.1016/j.ocecoaman.2017.02.023>
- Sunamura, T. (1982). A wave tank experiment on the erosional mechanism at a cliff base. *Earth Surface Processes and Landforms*, 1982(7), 333–343. <https://doi.org/10.1002/esp.3290070405>
- Sunamura, T. (1992). *The geomorphology of rocky coasts* (p. 302) Wiley.
- Sunamura, T. (2015). Rocky coast processes: With special reference to the recession of soft rock cliffs. *Proceedings of the Japan Academy Ser B Physical and Biological Sciences*, 91(9), 481–500. <https://doi.org/10.2183/pjab.91.481>
- Ulzega, A., Leone, F., & Orrù, P. (1986). Geomorphology of submerged Late Quaternary shorelines on the South Sardinian continental shelf. *Journal of Coastal Research Special Issue*, 1, 73–82.
- Young, A. P. (2018). Decadal-scale coastal cliff retreat in southern and central California. *Geomorphology*, 300, 164–175. <https://doi.org/10.1016/j.geomorph.2017.10.010>